IOP Conf. Series: Journal of Physics: Conf. Series **1012** (2018) 012007 doi:10.1088/1742-6596/1012/1/012007

Bending-Stiffness Dependent Generic Structural Transitions of Helical Polymers

Yifan Dai and Michael Bachmann

Soft Matter Systems Research Group, Center for Simulational Physics, Department of Physics and Astronomy, University of Georgia, Athens, GA 30605, USA

E-mail: dai@smsyslab.org, bachmann@smsyslab.org
Homepage: http://www.smsyslab.org

Abstract. We investigate the impact of competing bending and torsion effects upon the formation of structural phases for helical polymers. For this purpose, parallel-tempering replica-exchange simulations of a coarse-grained polymer model were performed and thermodynamic response quantities analyzed. Extremal energetic and structural fluctuations are used as indicators of significant phase changes. A systematic analysis of the phase structure supports earlier results suggesting the relevance of strong bending stiffness for the stabilization of helical phases. In addition, we find a novel phase at intermediate values of the bending stiffness that provides insight into the process of helix-bundle formation.

1. Introduction

Structural transitions of macromolecules can be considered thermodynamic phase transitions on mesoscopic scales. The conventional approach of analyzing fluctuation quantities such as the heat capacity to identify transition points can be directly employed, but for finite systems, no critical or otherwise catastrophic behavior is expected to occur. Therefore, it is more difficult to obtain a general picture of the phase structure in these systems. Nonetheless, much effort has been dedicated to understanding structural transitions in macromolecular systems of finite size in recent years, including the development of advanced statistical analysis methods [1].

In this paper, we discuss results of continued studies of linear, helical polymers. Helix formation can be induced by a torsion potential [2], which simulates the secondary-structure effects hydrogen bonds cause in real polymers. In addition, non-bonded monomers tend to interact with each other via van der Waals forces, which compete with local ordering achieved by the torsion restraints. As it has been shown, the resulting folded structures, which are supposed to be "functional" in biological systems (such as proteins), do not exhibit any order and look rather like amorphous solids. Apparently, an additional energetic contribution is needed to stabilize low-entropy helical structures such as helix bundles. It was found that a bending potential of two successive bonds indeed helps stabilize the ordered structures but still allows for tertiary structure effects like the formation of compact helix bundles [3, 4, 5].

Here, we investigate structural phase changes for a scenario, in which three-helix structures dominate in the ordered phase, stabilized by strong bending restraints. We systematically weaken the restraints and study the crossover from helical to amorphous compact structures, which govern the conformational behavior at low temperatures if bending restraints are absent.

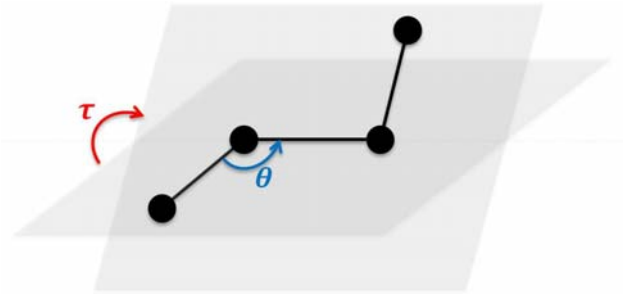

Figure 1. Four monomers are connected by three successive bonds. The bending angle is denoted by θ (blue) and the torsion angle by τ (red).

For this purpose, extensive parallel-tempering Monte Carlo simulations of a coarse-grained helical polymer model were performed [6, 7, 8].

2. Modeling and Simulation

2.1. Modeling

Complex macromolecules such as functional bioproteins are finite systems, which typically consist of thousands of atoms. However, the general structural behavior of macromolecules does not necessarily depend on atomistic details and the chemical group(s) forming a monomer can be considered a coarse-grained entity. Therefore, we employ a generic coarse-grained bead-spring model for an elastic homopolymer, in which individual monomers or chain segments possess only a small number of physical properties. Here, we focus on a model of a polymer chain with $N = 40$ monomers. It already exhibits a distinguished structural phase space, which makes it an ideal candidate for this systematic study.

The conformation of the polymer can be represented by the vector $\mathbf{X} = (\mathbf{x}_1, \mathbf{x}_2, ..., \mathbf{x}_{40})$ where $\mathbf{x}_i$ is the position of the ith monomer. The energy of the polymer chain includes non-bonded, bonded, bending, and torsional interactions. By combining all four potentials, a polymer with conformation $\mathbf{X}$ has the total energy [3, 4]

$$E(\mathbf{X}) = S_{\mathrm{LJ}} \sum_{i>j+1} U_{\mathrm{LJ}}(r_{ij}) + S_{\mathrm{FENE}} \sum_{i} U_{\mathrm{FENE}}(r_{ii+1}) + S_{\mathrm{bend}} \sum_{l} U_{\mathrm{bend}}(\theta_l) + S_{\mathrm{tor}} \sum_{k} U_{\mathrm{tor}}(\tau_k). \quad (1)$$

The interactions between all non-bonded monomers are represented by the dimensionless shifted Lennard-Jones (LJ) potential with cutoff,

$$U_{\mathrm{LJ}}(r) = \begin{cases} 4[(\sigma/r)^{12} - (\sigma/r)^6] - U_{\mathrm{LJ}}(r_c), & r \le r_c, \\ 0, & \text{otherwise.} \end{cases} \quad (2)$$

The van der Waals radius of a monomer is $\sigma = r_0/2^{1/6}$, where r_0 is the inter-monomer distance associated with the minimum of the LJ potential. We use r_0 as the basic length scale and set it to unity in the simulation. The cutoff distance $r_c = 2.5\sigma$ is introduced and the potential is shifted by $U_{\mathrm{LJ}}(r_c) = 4[(\sigma/r_c)^{12} - (\sigma/r_c)^6] \approx -0.0163169$ to avoid a discontinuity at the cutoff point. The non-bonded interaction strength S_{LJ} ($\equiv 1$ in the simulations) provides the reference energy scale for all energetic quantities.

Any pair of bonded monomers interact via the finitely extensible nonlinear elastic (FENE) potential [9, 10]

$$U_{\mathrm{FENE}}(r) = \ln\{1 - [(r - r_0)/R]^2\}, \quad (3)$$

where R is the parameter that limits minimum and maximum bond lengths. The FENE potential diverges as $r \to r_0 \pm R$. The bond interaction strength is $S_{\mathrm{FENE}} = -KR^2/2$ for which we use standard parameter values $K = (98/5)r_0^2$ and $R = (3/7)r_0$ [4].

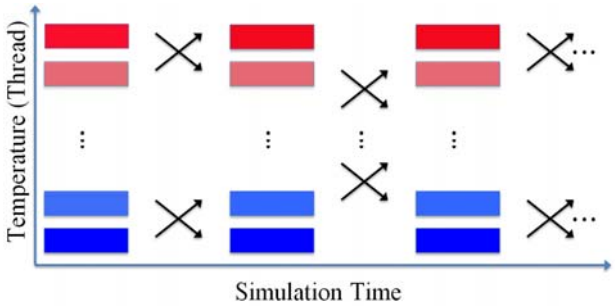

Figure 2. Alternating replica-exchange scheme. Red boxes represent high-temperature and blue boxes low-temperature threads. Arrows indicate the exchanges between neighbors. The first and last thread are idle during every other exchange.

The bending energy is given by

$$U_{\text{bend}}(\theta) = 1 - \cos(\theta - \theta_0), \tag{4}$$

where θ is the bending angle formed by two successive bonds (see Fig. 1). We set the reference bending angle to $\theta_0 = 1.742$.

Similarly, the torsional energy is given by [2]

$$U_{\text{tor}}(\tau) = 1 - \cos(\tau - \tau_0), \tag{5}$$

where τ is an out-of-plane angle formed by three successive bonds as shown in Fig. 1. The reference torsional angle is $\tau = 0.873$. With these preferences of θ_0 and τ_0, the polymer in our model resembles α-helices with about 4 monomers per turn in the ground state.

In recent studies, the structural phases for flexible ($S_{\text{bend}} = 0$) and semiflexible ($S_{\text{bend}} = 200$) polymers could be identified for a large array of torsion strengths S_{tor} [3, 4, 5]. However, the structural transition behavior for bending strengths S_{bend} between these limits has not yet been investigated systematically. We know from previous studies that there are major differences in the structural behavior of flexible and semiflexible polymers at low temperatures. Low-energy conformations of flexible polymers with 40 monomers are compact for $S_{\text{tor}} = 5$ and do not exhibit striking features of order. These structures were classified as amorphous solids. Contrarily, under the same conditions semiflexible polymers form 3-helix bundles, which resemble tertiary structures composed of helical segments as found in proteins. Upon heating, the compact structures melt and globular conformations dominate the "liquid" phase, whereas an additional liquid-gas transition destroys any remaining local structural order. Random-coil conformations govern the "gas" phase.

In this study, we systematically vary S_{bend} at constant torsional strength $S_{\text{tor}} = 5$ and investigate the crossover regime between the structural phases of flexible and semiflexible helical polymers described above.

2.2. Simulation and sampling

The standard importance-sampling technique typically used in Monte Carlo simulations is the Metropolis method, which is based on the canonical microstate probability $p(\mathbf{X}) \sim e^{-\beta E(\mathbf{X})}$ at the given temperature T ($\beta = 1/k_{\text{B}}T$). Thus the acceptance probability $P^{\text{MC}}_{\text{accept}}$ is governed by the ratio of the canonical weights of the microstates

$$P^{\text{MC}}_{\text{accept}}(\mathbf{X} \to \mathbf{X}') = \min\left(1, e^{-\beta \Delta E}\right), \tag{6}$$

where $\Delta E = E(\mathbf{X}') - E(\mathbf{X})$. A Monte Carlo displacement update from $\mathbf{X}$ to $\mathbf{X}'$ is proposed within a cubic box with edge lengths $d = 0.3r_0$. If the energy of the new microstate in each Cartesian direction is smaller after an update, $E(\mathbf{X}') < E(\mathbf{X})$, the move is accepted. If the

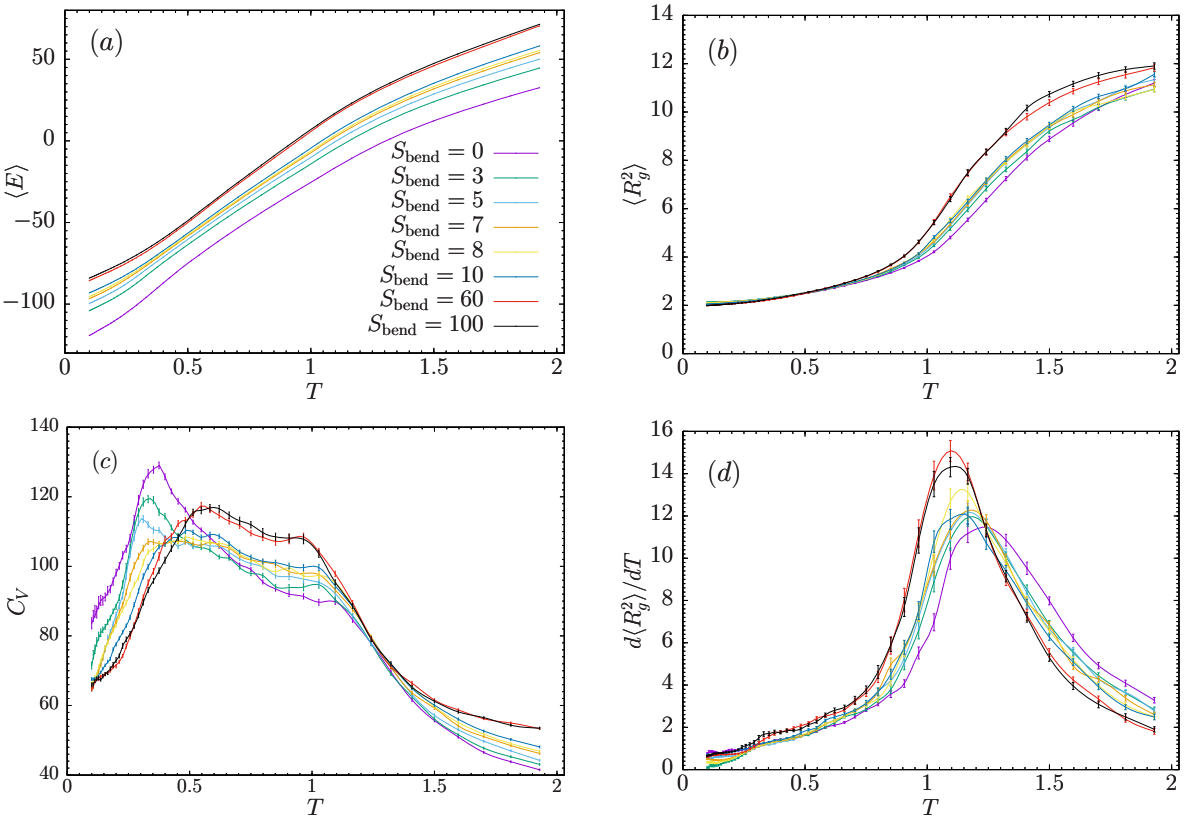

Figure 3. Mean values of (a) energy $\langle E \rangle$, (b) squared gyration radius $\langle R_g^2 \rangle$ and the corresponding fluctuation widths (c) heat capacity C_V, (d) $d\langle R_g^2 \rangle / dT$ as functions of temperature T at various bending strengths $S_{\rm bend}$ for a helical polymer with 40 monomers and torsion strength $S_{\rm tor} = 5$.

chosen update provokes an increase of energy, $E(\mathbf{X}') > E(\mathbf{X})$, the conformational change is accepted only with the probability $e^{-\beta \Delta E}$. However, the Metropolis method is also one of the least efficient methods due to the difficulty to overcome local free-energy barriers within a reasonable number of local moves. In order to enhance the sampling of low-energy configurations and improve the efficiency, we employ the replica-exchange Monte Carlo (parallel tempering) method [6, 7, 8]. In parallel tempering, multiple process threads are utilized where each thread corresponds to one temperature. After a sufficient number of Monte Carlo sweeps (~ 2000) have been performed, the configuration in each temperature thread is attempted to be exchanged with one of its neighbors. Since the first and last thread have only one neighbor, they remain idle among half of the exchanges. The exchange scheme is shown in Fig. 2. In our study we use 48 temperature threads in the interval $T \in [0.1, 2)$ where $T_i = 1.065\, T_{i-1}$. The acceptance probability $P_{\rm accept}^{\rm PT}$ for a single exchange between thread i and thread j is

$$P_{\rm accept}^{\rm PT} = \min \left(1, e^{-(\beta_i - \beta_j)[E(\mathbf{X}_j) - E(\mathbf{X}_i)]} \right). \tag{7}$$

Statistical errors of the quantities measured in the individual threads are calculated using the Jackknife error estimation method (for a description see, e.g., Ref. [1]).

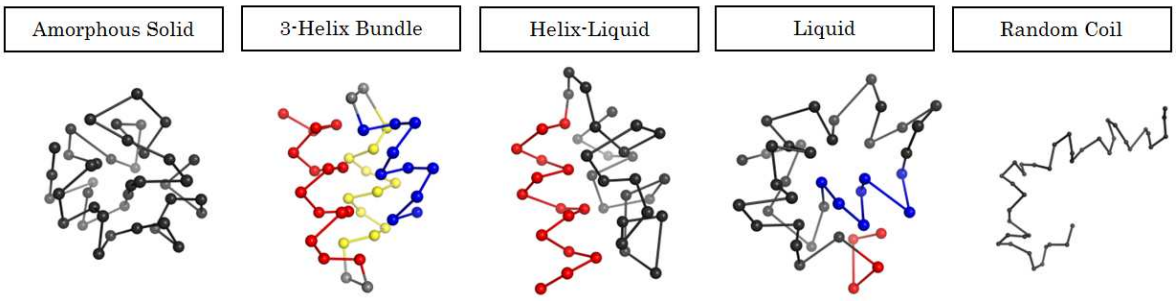

Figure 4. Representative conformations dominating the different structural phases identified for bending strengths in the interval $0 < S_{\text{bend}} < 200$ at $S_{\text{tor}} = 5$.

3. Results

For the investigation of the thermodynamic behavior of helical polymers with different bending strengths, we employ conventional canonical statistical analysis. Energetic and structural thermodynamic quantities were measured at the temperatures used in the parallel-tempering simulation and characteristic features such as inflection points, peaks, and "shoulders" in the curves are used as indicators of structural transitions. Because the system is finite, discontinuities do not occur and the temperatures, at which a specific transition signal is identified in different quantities, do not typically coincide. Therefore, the thermodynamic interpretation of the results is more qualitative than quantitative. Nonetheless, this approach is capable of revealing the most significant features of the transition behavior and the dependence on the bending stiffness.

The results for the general thermodynamic quantities obtained in our simulations at $S_{\text{tor}} = 5$ are compiled in Fig. 3. Shown are the mean energy $\langle E \rangle$ and mean squared radius of gyration $\langle R_g^2 \rangle$, as well as the corresponding thermal fluctuations $C_V = d\langle E \rangle / dT$ (heat capacity) and $d\langle R_g^2 \rangle / dT$ as functions of temperature for different bending strengths $S_{\text{bend}} \in [0, 100]$.

The limit $S_{\text{bend}} = 0$ is associated with flexible polymers and our results are in agreement with previous studies [4]. On the other end, $S_{\text{bend}} = 100$ represents a semiflexible helical polymer with strong bending restraints which stabilize helical conformations. For $S_{\text{tor}} = 5$ and $S_{\text{bend}} = 100$, the helical phase is dominated by 3-helix bundles. No noteworthy change in transition behavior occurs for larger bending strengths $S_{\text{bend}} > 100$. It is, therefore, appealing to take a closer look at intermediate values of S_{bend} and study the change in transition behavior when crossing over from flexible to semiflexible polymers.

The heat capacity shown in Fig. 3(c) exhibits two major transition signals for all bending strengths. The peaks near $T \approx 1$ (with small variations depending on S_{bend}) are supported by strong fluctuations in the radius of gyration [see Fig. 3(d)]. This is an indication that the transition causes major changes in the spatial dimension of the structures and can clearly be associated with the gas-liquid transition between globular and random, expanded conformations. The liquid phase of helical polymers is characterized by globular, overall disordered structures, which may contain short, locally ordered segments such as helical turns. The random-coil conformations do not exhibit any indication of order and the fluctuation behavior of the individual monomers is only constrained by the bond potential.

The other transition signal in the specific-heat curves, which for the different S_{bend} values is found in the interval $0.3 < T < 0.6$, is only weakly reflected in the fluctuations of the radius of gyration. This indicates that it is a transition between compact structures: the globular conformations above the transition temperature and the more ordered, but not necessarily

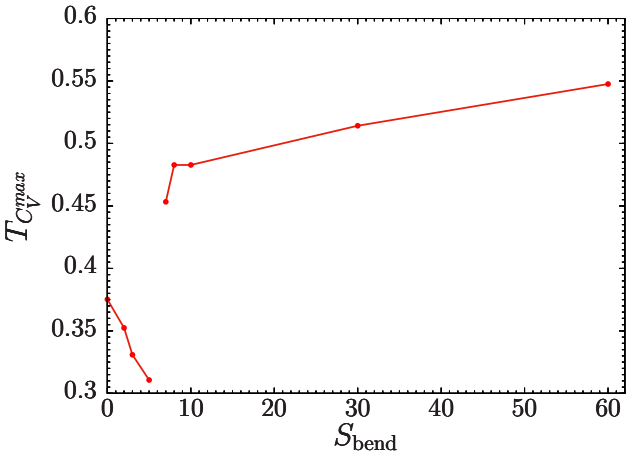

Figure 5. Dependence of the peak temperature of the heat capacity $T_{C_V^{\max}}$ on the bending strength S_{bend} for the compact phases.

denser, conformations at low temperatures. From the studies in the flexible and semiflexible limits, we know that for S_{tor} the low-energy conformations of flexible polymers are amorphous solids, whereas semiflexible helical polymers form very stable, highly ordered 3-helix bundles. Hence, whereas the transition can generically be referred to as the liquid-solid transition in both cases, the structural features in the solid phase are strikingly different. A representative example of an amorphous solid and a 3-helix bundle are shown in Fig. 4.

In order to understand better how these different solid phases are formed, it is helpful to investigate in more detail polymers with intermediate bending strengths. A closer look at the shift of the liquid-solid transition temperature gives a decisive hint. Using again the peak temperature of the heat capacity curves in the low-temperature regime, we observe that by increasing the bending stiffness S_{bend}, the transition point shifts to *lower* temperatures, while the peak height decreases. Then, at about $S_{\mathrm{bend}} = 5$, the signal has shifted to $T \approx 0.31$, but for $S_{\mathrm{bend}} = 7$ another signal appears at about $T \approx 0.45$. This signal becomes stronger for larger S_{bend} values and shifts to *higher* temperatures. Figure 5 shows how the peak locations change with S_{bend}. The "gap" between the signals is clearly visible. This behavior gives rise to the assumption that an intermediate phase exists for $5 < S_{\mathrm{bend}} < 7$, which mediates the crossover between amorphous and helical structures. Indeed, by visual inspection of the dominant structures, we find a new structure type which has not been observed in the limiting cases of flexible and semiflexible polymers. It is a compact and hybrid "helix-liquid" structure, which possesses an ordered helical segment attached to a disordered ("liquid") body. This intermediate structural phase is rather weak and occurs only for bending strengths $S_{\mathrm{bend}} = 5 \ldots 7$ (at $S_{\mathrm{tor}} = 5$). However, it shows how helical bundles form out of the liquid phase, provided the bending stiffness is sufficiently strong to counter the non-bonded interactions that cause the formation of most compact amorphous (or crystalline) structures.

4. Summmary

We have performed parallel-tempering Monte Carlo simulations of a coarse-grained model of helical polymers, in which non-bonded and bonded pair interactions compete with multi-body bending and torsion potentials. For a specific scenario, in which the solid structural phase of semiflexible polymers is governed by 3-helix bundles and by amorphous, solid structures for flexible polymers, we modify the bending stiffness systematically to understand the significant difference in the shapes of the solid structures. Canonical statistical analysis of energetic and structural fluctuation quantities reveals that another structural phase exists in a certain intermediate interval of bending stiffness values, where conformations are composed of a single helix attached to a disordered "liquid" body. Future studies on the characteristic

and quantitative features of this intermediate phase are necessary to understand better the general consequences for folding processes of polymer chains under the influence of competing interactions and constraints.

5. Acknowledgments

We thank Dr. Matthew J. Williams for helpful comments. The project was supported by the National Science Foundation (NSF) under Grant No. DMR-1463241.

References

[1] Bachmann M 2014 *Thermodynamics and Statistical Mechanics of Macromolecular Systems* (Cambridge: Cambridge University Press)
[2] Rapaport D C 2002 *Phys. Rev. E* **66** 011906
[3] Williams M J and Bachmann M 2015 *Phys. Rev. Lett.* **115** 048301
[4] Williams M J and Bachmann M 2016 *Phys. Rev. E* **93** 062501
[5] Williams M J and Bachmann M 2016 *Polymers* **8** 245
[6] Swendsen R H and Wang J S 1986 *Phys. Rev. Lett.* **57** 2607
[7] Geyer C J 1991 *Computing Science and Statistics: Proceedings of the 23rd Symposium on the Interface* edited by Keramidas E M (Fairfax Station, VA: Interface Foundation)
[8] Hukushima K and Nemoto K 1996 *J. Phys. Soc. Jpn.* **65** 1604
[9] Kremer K and Grest G S 1990 *J. Chem. Phys.* **92** 5057
[10] Milchev A, Bhattacharya A, and Binder K 2001 *Macromolecules* **34** 1881